

# Semi-controlled rectifier for output power regulation of series-series compensated inductive power transfer systems

ELENI GATI, ALEXANDROS MOIROPOULOS and STEFANOS MANIAS

Department of Electric Power  
School of Electrical & Computer Engineering  
National Technical University of Athens  
9 Iroon Polytexneiou St., 15780 Zografos  
GREECE  
gatiel@mail.ntua.gr

*Abstract:* - In this work, a semi-controlled rectifier is proposed for the secondary side of a series-series compensated inductive power transfer system, in order to regulate the power provided to the load. The control strategy is based on dynamic mode change between the conventional full-wave rectification and asymmetric loading, in order to reach and maintain the desirable output power. The asymmetric loading mode of operation leads to up to four times higher output power than conventional full-wave rectification. This allows for a wide range of output power regulation. Simulation results show a good response to pre-set values or characteristics and steady output power. The proposed rectifier is suitable for wireless chargers with wide output power specifications.

*Key-Words:* - inductive charger, asymmetric loading, resonant circuit, output power control, wireless power transfer

## 1 Introduction

Wireless power transfer through inductive coupling is steadily gaining popularity in low and high power charging applications ranging from electrical and electronic appliances to electric vehicle contactless chargers.

In inductive power transfer systems (IPTs), power is transferred through the magnetic field that links two or more coupled coils, when the primary coil is excited by a high frequency source. Due to the high air gap characterizing the majority of these systems, weak coupling conditions are encountered. Since power transfer capability depends on the coupling coefficient,  $k$ , between the transmitter and receiver coils, and  $k$  is commonly well below 0.6 in such applications, compensating capacitors are incorporated in various topologies in both sides of the system. Operation of the L-C topologies close to resonance ensures compensation of the high leakage inductances and allows for significant power transfer [1].

However, power transfer is also load dependent. Large load resistances reduce the quality factor of the series resonant circuits, resulting in a deterioration of their power transfer capability.

Ongoing research is focusing on solutions for transferring power through large air gaps, low and variable coupling conditions, caused by

misalignment between the coupled coils and power or efficiency optimization [2],[3].

Output power control in IPTs can be performed either from the primary side, or from the secondary side of the system. In the first case, control is achieved by variation of the inverter duty-cycle [4],[5] or the conduction phase [6], while the frequency of operation is maintained fixed. In the second case, load transformation is performed with an additional dc/dc converter stage [7],[8] or duty-cycle/ phase control of a controlled rectifier [9] is implemented.

In this work, output power control is performed at the secondary side of a series-series compensated IPTs via a semi-controlled rectifier. A simple control strategy is proposed, on the basis of transition between two modes of operation of the system; the conventional full-wave rectification mode and the asymmetric loading mode. Asymmetric loading has been proposed and analysed in [10] and [11] and refers to a half-cycle loading and half-cycle short-circuit of the system. This mode of operation leads to an increased output power compared to full-wave rectification. With the proposed converter, variation of the output power of the system through a wide range is possible, with no reduction in the efficiency of the system, since soft-switching conditions are maintained.

In Section 2, the series-series compensated IPTS is introduced and an analysis of its operation with full-wave rectification and asymmetric loading is presented. In Section 3, simulation results are recorded for various states of operation of the proposed converter.

## 2 Series-series Compensated Inductive Power Transfer System

The series-series (SS) compensated topology is selected in high power IPTSs for its voltage source characteristics.

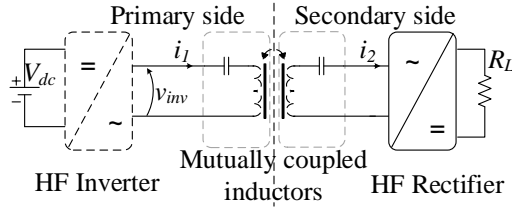


Fig. 1. Block diagram of series-series compensated Inductive Power Transfer System.

In this topology, illustrated in Fig. 1, the compensating capacitors are connected in series with the primary (transmitter) and secondary (receiver) coils. For the mathematical analysis of this system, first harmonic approximation is performed, assuming that for operation close to resonance, power transfer is achieved through the fundamental frequency of operation. The leakage equivalent circuit of the SS IPTS is depicted in Fig. 2, where  $L_1$  and  $L_2$  are the primary and secondary coil inductances, respectively,  $C_1$  and  $C_2$  the primary and secondary compensating capacitors,  $M$  is the mutual inductance,  $R_1$  and  $R_2$  are the internal resistances of the resonant circuits,  $R_{ac}$  is the reflected load to the ac side of the secondary and  $v_{inv,1}$  is the first harmonic of the inverter output voltage. The leakage inductances are  $L_{11}=L_1-M$  and  $L_{12}=L_2-M$ .

By transforming it to its Thevenin equivalent, with the use of relations (1)-(6), the frequency of operation for which the system operates as a voltage source is obtained in (7). Assuming  $L_1=L_2=L$  and  $C_1=C_2=C$  and considering internal resistances  $R_1, R_2$  as negligible, the frequency of operation for unity voltage gain becomes equal to (8). For operation at  $\omega_1$ ,  $v_{TH}$  becomes equal to  $v_{inv,1}$ . Therefore, the output power of the system is equal to (9).

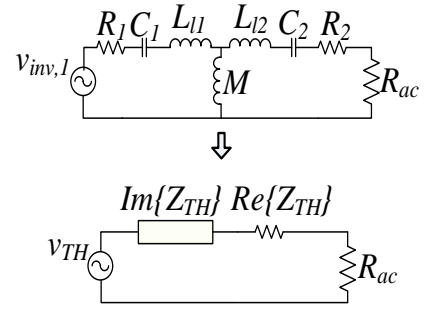


Fig. 2. Block diagram of series-series compensated Inductive Power Transfer System.

$$Z_1 = R_1 + \frac{1}{j\omega C_1} + j\omega L_1 \quad (1)$$

$$Z_2 = R_2 + \frac{1}{j\omega C_2} + j\omega L_2 \quad (2)$$

$$Z_{TH} = Z_2 + \frac{\omega^2 M^2}{Z_1} \quad (3)$$

$$v_{TH} = \frac{j\omega M}{Z_1} v_{inv,1} \quad (4)$$

$$\Re\{Z_{TH}\} = \frac{R_1(R_1 R_2 + \omega^2 M^2) + R_2\left(\omega L_1 - \frac{1}{\omega C_1}\right)^2}{R_1^2 + \left(\omega L_1 - \frac{1}{\omega C_1}\right)^2} \quad (5)$$

$$\Im\{Z_{TH}\} = \frac{R_1^2\left(\omega L_2 - \frac{1}{\omega C_2}\right) + \left(\omega L_1 - \frac{1}{\omega C_1}\right)\left[\left(\omega L_1 - \frac{1}{\omega C_1}\right)\left(\omega L_2 - \frac{1}{\omega C_2}\right) - \omega^2 M^2\right]}{R_1^2 + \left(\omega L_1 - \frac{1}{\omega C_1}\right)^2} \quad (6)$$

$$\Im\{Z_{TH}\} = 0 \Rightarrow \omega_{1,2} = \sqrt{\frac{\frac{L_2}{C_1} + \frac{L_1}{C_2} \pm \sqrt{\left(\frac{L_2}{C_1} - \frac{L_1}{C_2}\right)^2 + \frac{4M^2}{C_1 C_2}}}{2(L_1 L_2 - M^2)}} \quad (7)$$

$$\omega_1 = \sqrt{\frac{1}{CL(1-k)}} \quad (8)$$

$$P_o = \tilde{I}_2^2 R_{ac} = \frac{\tilde{V}_{inv,1}^2}{R_{ac}} \quad (9)$$

In the following sub-section, the output power of a series-series compensated IPTS is evaluated for two different rectification topologies in the secondary side of the system; full-wave rectification and the asymmetric loading topology.

### 2.1 Full-wave rectification and Asymmetric loading

In a full-wave rectification, which is the conventional rectifying topology in IPTSs, the load is connected to the source for the whole period of operation of the system. This can be considered as a symmetric loading of the driving circuit.

On the other hand, asymmetric loading, as proposed in [11], entails connection of the load to the source only for half the cycle of operation. The latter was implemented with the use of a diode in parallel with the load resistance, as shown in Fig. 3.

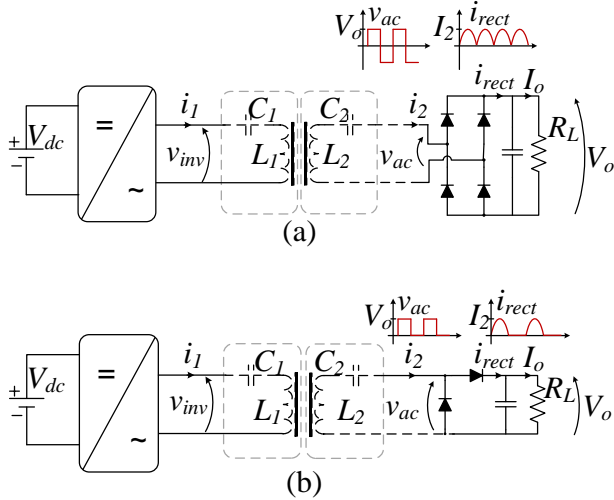


Fig. 3. SS IPTS with (a) full wave rectification and capacitive output filter and (b) asymmetric loading topology and capacitive output filter.

Theoretical analysis of this topology, including the effect of the capacitive output filter [12], shows a possible increase of up to four times in the output power compared with the one achieved with the use of a conventional full-wave rectifier with the same output filter. This increase is caused by the reduction of the value of the load resistance as reflected to the source, which leads to an increase in the quality factor of the resonant circuit, resulting in higher power intake from a given voltage source.

The maximum gain can be achieved when the system operates at the resonant frequency \$\omega\_1\$ and the internal resistances of the resonant circuits are negligible.

More specifically, the reflected load to the ac side of the system can be evaluated in each case with the help of the voltage and current waveforms depicted in Fig. 3, by using eq. (10), since current \$i\_2\$ is sinusoidal. Calculations yield the reflected ac load for full-wave rectification as in (11) and for asymmetric loading operation in (12). By replacing these values to (9), the output power is obtained in (13) for full-wave rectification and in (14) for the asymmetric

loading topology. The ratio of the output power for these two topologies is evaluated in (15) and is equal to four.

$$R_{ac} = \frac{\tilde{V}_{ac,l}}{\tilde{I}_2} \tag{10}$$

$$R_{ac, fw} = \frac{\tilde{V}_{ac, fw,l}}{\tilde{I}_{2, fw}} = \frac{\frac{2\sqrt{2}}{\pi} V_{o, fw}}{\frac{\pi}{2\sqrt{2}} I_{o, fw}} = \frac{8}{\pi^2} R_L \tag{11}$$

$$R_{ac, as} = \frac{\tilde{V}_{ac, as,l}}{\tilde{I}_{2, as}} = \frac{\frac{2}{\pi\sqrt{2}} V_{o, as}}{\frac{\pi}{\sqrt{2}} I_{o, as}} = \frac{2}{\pi^2} R_L \tag{12}$$

$$P_{o, fw} = \frac{\tilde{V}_{inv,l}^2}{\frac{8}{\pi^2} R_L} = \frac{\pi^2 \tilde{V}_{inv,l}^2}{8 R_L} \tag{13}$$

$$P_{o, as} = \frac{\tilde{V}_{inv,l}^2}{\frac{2}{\pi^2} R_L} = \frac{\pi^2 \tilde{V}_{inv,l}^2}{2 R_L} \tag{14}$$

$$\frac{P_{o, as}}{P_{o, fw}} = 4 \tag{15}$$

In real-life systems, where internal resistances are present, the actual power ratio becomes lower than four, as the ratio of \$R\_{ac}/ Re\{Z\_{TH}\}\$ decreases. The gain increases with the load resistance due to the improvement in the system quality factor, caused by the significant reduction in the reflected resistance. In any case, for operation close to \$\omega\_1\$, a significant power gain can be obtained with asymmetric loading. Additionally, as described in [11] and [12], the efficiency of the system with asymmetric loading is better than that of the full-wave rectification for medium and high resistance values, for operation close to resonance.

### 2.2 Semi-controlled rectifier topology

Both the conventional full-wave rectifier and the asymmetric loading circuits are passive topologies, which do not allow for output control in the secondary side of the IPTS. If either of them is selected for the implementation of an inductive charger, output power control can only be implemented either by primary-side control, or by adding an extra dc/dc conversion stage after the rectifier in the secondary side.

However, it is possible to controllably take advantage of the output power gain that can be achieved by employing the asymmetric loading topology compared to the full-wave rectification, by

using a semi-controlled rectifier. With the appropriate driving signals, the system can in real-time switch between full-wave rectification and asymmetric loading so as to achieve a predetermined, or a varying output power level. Thus, output power control can be performed at the secondary side of the system, without interfering with the inverter frequency of operation or adding conversion stages to the system.

The proposed topology for the semi-controlled rectifier is depicted in Fig. 4. By replacing one of the four diodes of the conventional full-wave rectifier with a semiconductor switch, the asymmetric loading mode can be controllably achieved. No activation of the switch results in a typical full-wave rectification, with the modes of operation presented in Fig. 5 (a) and (b). When the required output power is higher than the one obtained with full-wave rectification, a transition to asymmetric loading can occur. In this case, the modes of operation are depicted in Fig. 5 (c) and (d).

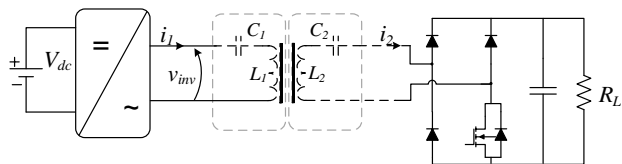


Fig. 4. SS IPTS with semi-controlled rectifier in the secondary side.

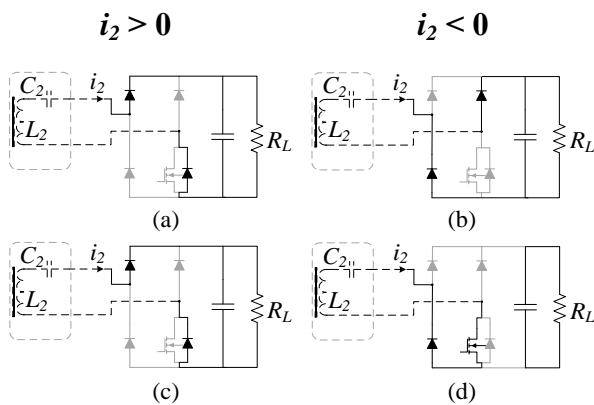


Fig. 5. Modes of operation of the semi-controlled rectifier.

The proposed control block diagram is presented in Fig. 6. The power provided to the load is measured and compared to the desirable predetermined level. Then the controller activates the switch in order to set the system to the asymmetric loading mode the time intervals necessary to reach the pre-set output power. In order for the proper driving of the switch, the secondary current,  $i_2$ , is sensed so that a driving pulse

is available for the switch during each negative half-cycle of operation.

For achieving soft switching of the semiconductor it must be ensured that the sensing and control duration for each cycle of operation is shorter than the turn-on time of the diodes. Otherwise, the diodes will conduct before the switch, and the activation of the switch will be made in hard-switching conditions.

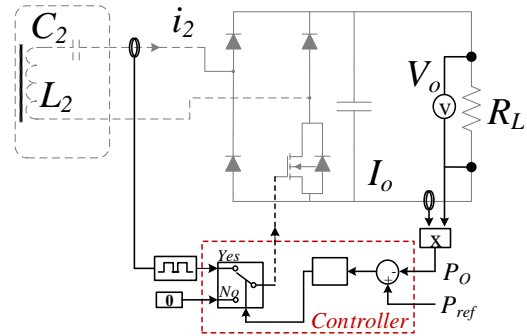


Fig. 6. Block diagram of the proposed control scheme.

### 3 Simulation Results

The proposed topology is simulated using the Matlab/ Simulink platform. The component values used for the simulation are listed in Table 1.

Table 1. Simulation parameters

Parameter	Value	Parameter	Value
$L_1$	180 $\mu$ H	$C_1$	18.8 nF
$L_2$	180 $\mu$ H	$C_2$	18.8 nF
$k$	0.25	$R_L$	50 $\Omega$
$V_{in,DC}$	100 V	$f$	99.902 kHz

#### 3.1 Comparison between full-wave rectification and asymmetric loading

Simulations are carried out for the two topologies under examination; full-wave rectification and asymmetric loading, separately, for comparison reasons. The output power recorded for each case is  $P_{o,as} = 726.3$  W and  $P_{o,fw} = 190.3$  W. The internal resistances of the semiconductors and coils were included in the simulations.

Fig. 7 (a) shows the inverter output waveforms (in red) and inputs of the asymmetric loading (blue) and full-wave rectification (black) topologies, respectively. It is also observed that the voltage at the input of the asymmetric load topology has a minimum value of zero and a maximum greater than the amplitude of the output voltage of the inverter.

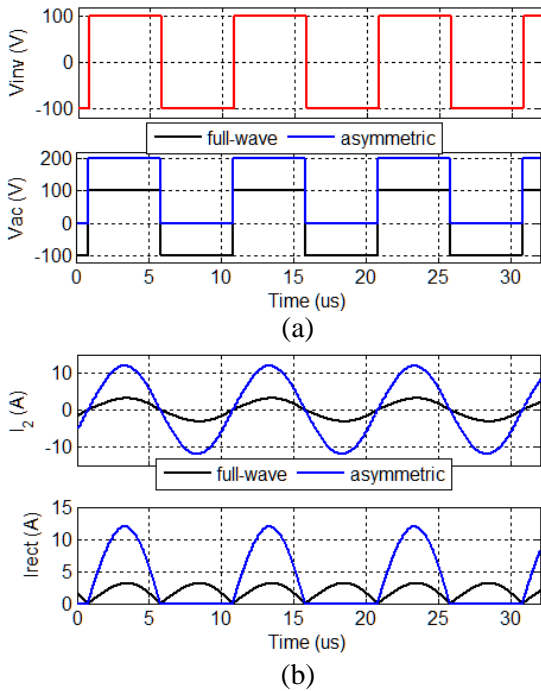


Fig. 7. (a) Inverter output voltage (red) and rectifier input voltage for asymmetric loading and full-wave rectification. (b) Rectifier input current,  $i_2$ , and output current,  $i_{rect}$ , for asymmetric loading and full-wave rectification.

Fig. 7 (b) depicts the secondary current and the rectification output current for asymmetric loading and full-wave rectification, respectively. It is noted that the output current of the asymmetric loading topology has, as expected, a half-wave form. It is worth noticing the difference in the magnitudes of the currents, under the same input voltage and the same dc-load. This is due to the load resistance transformation, explained in Section 2.1.

### 3.2 Results of the proposed control scheme

Before implementing the proposed output power regulation scheme, the range of the output power, determined by the output power for full-wave rectification and asymmetric loading, can be either calculated or evaluated through simulations.

Thus, setting any value between these two to the controller, results in a different ratio of transitions between full-wave rectification and asymmetric loading, for reaching the desired output power,  $P_{set}$ .

For  $P_{set} = 400$  W, the output of the system is illustrated in Fig. 8. The system reaches the pre-set value of output power in approximately 12 ms and maintains it thereafter. Fig. 9 presents a small time interval of the steady-state operation of the system. As can be seen, the output power ripple is 1.5% of the pre-set value.

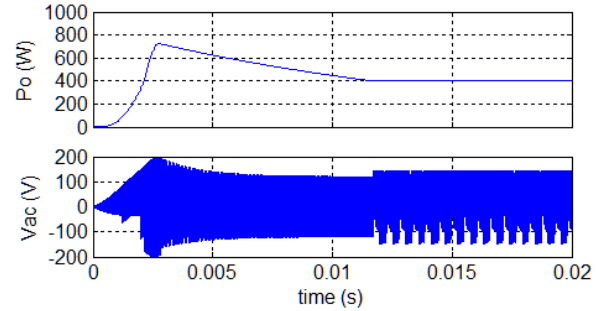


Fig. 8. Simulation results for  $P_{set} = 400$  W. Top: output power, bottom: waveform of the rectifier input voltage,  $v_{ac}$ .

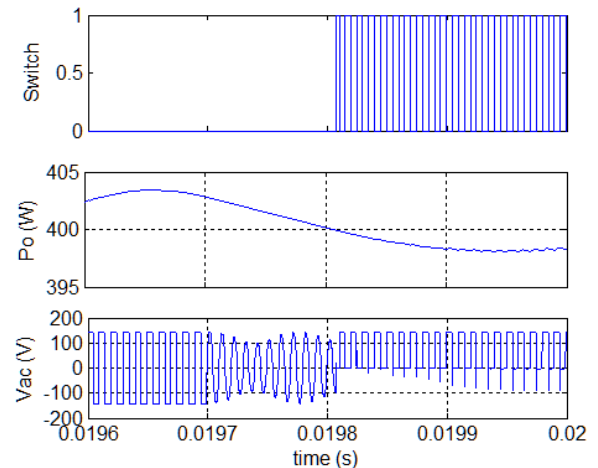


Fig. 9. Simulation results for  $P_{set} = 400$  W. Top: switch driving signal, middle: output power, bottom: waveform of the rectifier input voltage,  $v_{ac}$ .

In Fig. 10, the system response to various values of  $P_{set}$  is recorded. It is worth noticing that the output power ripple ranges from 1.5% to 3% of  $P_{set}$ , depending on how close the pre-set value is to either end of the power range. This is due to the dual nature of the system operation, based on which, two levels of output power are combined,  $P_{o, fw}$  and  $P_{o, as}$ , at different ratios for creating the desired average output power.

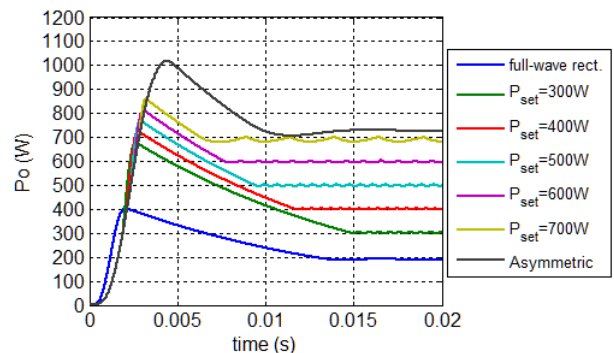


Fig. 10. Simulation results for various values of  $P_{set}$ .

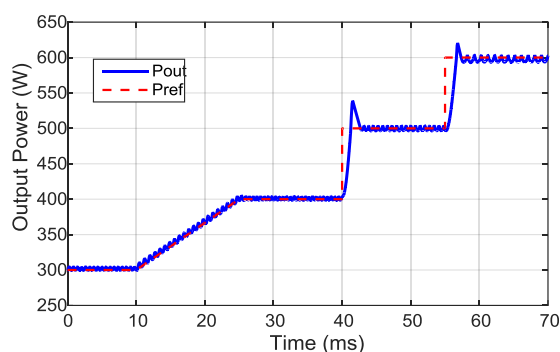


Fig. 11. Simulation results of output power following a reference characteristic.

The proposed control can be used for battery charging with predefined voltage/current or power characteristics. An example of following a pre-set characteristic is presented in Fig. 11, where the reference characteristic,  $P_{ref}$ , illustrated with the red line follows initially a ramp and then step transitions for the output power. The proposed controller tracks accurately the ramp and displays satisfactory response to the step changes of the output power.

## 4 Conclusion

In this work, a semi-controlled rectifier was proposed for the implementation of output power control in series-series compensated inductive power transfer systems. The proposed control scheme implements dynamic mode change between conventional full-wave rectification and asymmetric loading in order to reach and maintain a desirable output power level within the range  $\{P_{o,fw} - 4 \cdot P_{o,fw}\}$ . This strategy takes advantage of the wide difference in output power between the two modes of operation.

Simulation results showed good response to pre-set output power levels and power characteristics. The proposed semi-controlled rectifier employs a simple yet robust control scheme and can be used in battery charging applications of low or high power systems.

## Acknowledgement

Dr. E. Gati is financially supported for her Post-Doctoral research by the "IKY Fellowships of Excellence for Postgraduate Studies in Greece - Siemens Program 2016-2017".

## References:

[1] K. Yamaguchi, T. Hirata, Y. Yamamoto, I. Hodaka, Resonance and Efficiency in Wireless Power Transfer System, *WSEAS Transactions*

*on Circuits and Systems*, vol. 13, 2014, pp. 218-223.

- [2] N. Jamal, S. Saat, Y. Yusmarnita, A Development of Class E Converter Circuit for Loosely Coupled Inductive Power Transfer System, *WSEAS Transactions on Circuits and Systems*, Vol. 13, 2014, pp. 422-428.
- [3] Y. Yamamoto, K. Yamaguchi, T. Hirata, I. Hodaka, Feedback Effect for Wireless High-power Transmission, *WSEAS Transactions on Circuits and Systems*, vol. 13, 2014, pp. 241-245.
- [4] B. Peschiera, K. Aditya, S. S. Williamson, Asymmetrical voltage-cancellation control for a series-series fixed-frequency inductive power transfer system, *40th Annual Conference of the IEEE Industrial Electronics Society (IECON)*, 2014, pp. 2971-2977.
- [5] U. K. Madawala, D. J. Thrimawithana, A single controller for inductive power transfer systems, *35th Annual Conference of IEEE Industrial Electronics (IECON)*, 2009, pp. 109-113.
- [6] A. Namadmalan, Self-Oscillating Tuning Loops for Series Resonant Inductive Power Transfer Systems, *IEEE Trans. on Power Electronics*, vol. 31, no. 10, 2016, pp. 7320-7327.
- [7] M. Fu et al., Analysis and Tracking of Optimal Load in Wireless Power Transfer Systems, *IEEE Trans. on Power Electronics*, vol. 30, no. 7, 2015, pp. 3952-3963.
- [8] T. Hiramatsu, et al., Wireless charging power control for HESS through receiver side voltage control, *IEEE Applied Power Electronics Conference and Exposition (APEC)*, 2015, pp. 1614-1619.
- [9] K. Colak et al., A Novel Phase-Shift Control of Semibridgeless Active Rectifier for Wireless Power Transfer, *IEEE Trans. on Power Electronics*, vol. 30, no. 11, 2015, pp. 6288-6297.
- [10] E. Gati, S. Manias. Asymmetric loading of a series resonant R-L-C circuit for power transfer increase in inductive chargers, *39th Annual Conference of the IEEE Industrial Electronics Society (IECON)*, 2013, pp. 4570-4575.
- [11] E. Gati, G. Kampitsis, S. Manias, Output power increase of a series-series compensated inductive power transfer system via asymmetric loading, *17th European Conference on Power Electronics and Applications, EPE-ECCE Europe*, 2015.
- [12] E. Gati, S. Manias, Capacitive Output Filter Effect on Series-Series Inductive Power Transfer Systems Operating in Asymmetric Loading Mode, *in review*